THE JOURNAL OF BIOLOGICAL CHEMISTRY VOL. 281, NO. 45, pp. 34104–34112, NOVEMBER 10, 2006

Identification of a Filamin Docking Site on PTP-PEST*

Received for publication, June 30, 2006, and in revised form, September 12, 2006 Published, JBC Papers in Press, September 14, 2006, DOI 10.1074/jbc.M606277200

Martin P. Playford‡, Patrick D. Lyons‡, Sarita K. Sastry§, and Michael D. Schaller‡¶‖[1]

From the ‡Department of Cell and Developmental Biology, ¶Lineberger Comprehensive Cancer Center, and ‖Carolina Cardiovascular Biology Center, University of North Carolina at Chapel Hill, Chapel Hill, North Carolina 27599 and the §Sealy Center for Cancer Cell Biology, The University of Texas Medical Branch, Galveston, Texas 77555

PTP-PEST is a cytoplasmic protein-tyrosine phosphatase (PTP) implicated in the regulation of biological processes such as cell motility, cytokinesis, focal adhesion disassembly, and lymphocyte activation. Using a proteomics approach, filamin-A was identified as a novel interacting protein that bound to GST-PTP-PEST. This interaction was confirmed *in vitro* and in cells by coimmunoprecipitation. The site of filamin interaction on PTP-PEST was mapped to the fourth proline-rich region (Pro4). PTP-PEST has previously been implicated in the regulation of cytokinesis. In further support of this finding, expression of PTP-PEST in HeLa cells resulted in the formation of multinucleated cells. A PTP-PEST mutant lacking Pro4 and unable to bind filamin-A failed to induce the multinucleated phenotype. Further, depletion of filamin-A in HeLa cells was found to reduce the PTP-PEST-dependent multinucleation phenotype. Hence, we conclude that the interaction of PTP-PEST with filamin-A may function in the control of cytokinesis in mammalian cells.

Protein-tyrosine phosphatase (PTP)[2]-PEST, PTP-HCSF/BDP, and LYP/PEP comprise a small family of non-receptor PTPs (1). PTP-PEST is ubiquitously expressed, whereas PTP-HCSF/BDP1 and LYP/PEP are restricted in expression to hematopoetic tissue, although PTP-HCSF/BDP1 is also expressed in the brain (2–4). Ablation of PTP-PEST expression in the mouse results in embryonic lethality, demonstrating that this is an essential gene (5). PTP-PEST and related phosphatases have been implicated as negative regulators of B and T cell signaling, in part by controlling cytoskeletal changes required for lymphocyte function (6, 7). In non-lymphoid cells, PTP-PEST regulates cell migration. Interestingly, overexpression of PTP-PEST and ablation of PTP-PEST expression results in the same phenotype, impairment of cell migration (5, 8, 9). These findings suggest that perturbation of phosphotyrosine homeostasis with an excess or deficiency of PTP-PEST retards cell movement. PTP-PEST controls cell motility by regulating membrane protrusion via modulating the activity of Rac (9, 10). One other interesting phenotype exhibited by PTP-PEST-null cells is an apparent defect in cytokinesis (5). The mechanism by which PTP-PEST might control cytokinesis is undefined, but is postulated to involve a PTP-PEST associated protein, PSTPIP, which localizes to the cleavage furrow (11).

The PEST family of PTPs contains an N-terminal catalytic domain and a large C-terminal domain with numerous PEST and proline-rich sequences. These sequences function as docking sites for a number of proteins. PTP-PEST family binding partners include two adaptor proteins, Grb2 and Shc (12, 13), three focal adhesion-associated scaffolding proteins, Cas, paxillin, and the paxillin-related protein, hic-5 (14–17), the protein-tyrosine kinase, Csk (18, 19), and the cleavage furrow-associated protein, PSTPIP (11). The primary function of these interactions is apparently to recruit tyrosine-phosphorylated substrates into complex with PTP-PEST to facilitate their dephosphorylation (14, 20–22).

Given the role of the C-terminal noncatalytic domain of PTP-PEST in directing protein dephosphorylation by the direct and indirect recruitment of substrates into complex, we sought to further elucidate PTP-PEST function by identifying additional C-terminal domain binding partners. The actin-binding protein filamin-A was identified as a PTP-PEST associated protein using a proteomics approach. Filamin-A is a 280-kDa actin-binding protein (also known as ABP280) containing a pair of N-terminal calponin homology domains, which function to bind actin. Filamin-A cross-links filamentous actin into a branched orthogonal meshwork *in vivo* (23, 24). C-terminal to the actin binding domains are 24 repeats of a 96 amino acid motif, which serve as docking sites for many other proteins, including a number of signaling molecules like Rho family proteins and MKK4 (25, 26). Thus filamin-A is also envisioned to perform a signaling function by serving as a scaffold to tether signaling molecules (23, 24). PTP-PEST is the first identified tyrosine phosphatase that associates with filamin-A. The fourth proline rich region of PTP-PEST was found to mediate filamin-A binding and was also required for the induction of a multinucleated phenotype upon exogenous expression of PTP-PEST in HeLa cells, suggesting that docking with filamin-A might facilitate one of the biological functions controlled by PTP-PEST.

EXPERIMENTAL PROCEDURES

Cells—HEK 293 and 293T cells were maintained in Dulbecco's modified Eagle's medium (DMEM)/Ham's F-12 medium containing 10% fetal bovine serum and HeLa cells in DMEM

* This project was supported by National Institutes of Health Grant CA90901 and HL45100 (to M. D. S.). The costs of publication of this article were defrayed in part by the payment of page charges. This article must therefore be hereby marked "*advertisement*" in accordance with 18 U.S.C. Section 1734 solely to indicate this fact.

[1] To whom correspondence should be addressed: 534 Taylor Hall, CB 7090, Dept. of Cell & Developmental Biology, University of North Carolina at Chapel Hill, Chapel Hill, NC 27599. Tel.: 919-966-0391; Fax: 919-966-1856; E-mail: crispy4@med.unc.edu.

[2] The abbreviations used are: PTP, protein-tyrosine phosphatase; PBS, phosphate-buffered saline; DAPI, 4′,6-diamidino-2-phenylindole; GST, glutathione *S*-transferase; YFP, yellow fluorescent protein; GFP, green fluorescent protein.

containing 10% fetal bovine serum. 293T cells were transfected using the calcium phosphate method using 10 μg of DNA per 10-cm tissue culture plate (27). HeLa cells were transfected using TransIT-TKO according to the manufacturer's recommendation (Mirus, Madison, WI). Cells (7.5×10^5) were plated in a 6-cm tissue culture plate and incubated overnight at 37 °C prior to transfection. Routinely, 30 μl of TransIT-TKO were incubated with 7.5 μg of DNA in 750 μl of serum-free DMEM for 10 min prior to addition to the cells. Adenovirus constructs were generous gifts from Dr. Joan Taylor (UNC) and Dr. Mark Sussman (San Diego State University). The control and filamin (SMARTpool™) siRNA were purchased from Dharmacon (Lafayette, CO). For adenovirus infection, 2×10^6 cells were incubated with 30 PFU/cell at 37 °C for 24 h. Experiments were performed 72-h postinfection. For metabolic labeling, cells were grown to 80% confluence, washed with serum-free medium, then incubated overnight in methionine- and cysteine-free medium containing 10% conditioned media and 1.25 mCi ^{35}S-Translabel (MP Biomedicals, Inc, Irvine CA). Cell cultures were viewed in phase contrast using a Nikon TMS inverted microscope and imaged using a Nikon Coolpix 950 digital camera (×100 magnification).

Fluorescence Microscopy and Flow Cytometry—For expression analysis of YFP fusion proteins, HeLa cells were fixed in 3.7% formaldehyde for 10 min, washed once in phosphate-buffered saline (PBS), then incubated with PBS containing 100 ng/ml 4,6-diamino-2-phenylindole (DAPI) (Molecular Probes, Eugene, OR) for 3 min. The cells were washed once more in PBS, and mounted in a mixture of 10% Tris, pH 7.5, 90% glycerol, and 25 mg/ml 1,4-diazabicyclo (2,2,2)octane (DABCO) (Sigma). Immunostaining with filamin-A (1:500-Chemicon International, Victoria BC), PTP-PEST (1:100-Exalpha Biologicals, Maynard, MA), and β-tubulin (1:100 Sigma) monoclonal antibodies was performed on ice-cold 100% methanol-fixed cells (5 min room temperature) followed by DAPI staining and mounting as described above. For analysis by flow cytometry, trypsinized HeLa cells were washed once in PBS, resuspended in 500 μl of PBS, and fixed by addition of 315 μl of 95% ice-cold ethanol. The cells were stored at −20 °C until analysis. One hour prior to flow cytometry, the cells were pelleted by centrifugation at $1000 \times g$ for 5 min, washed once in PBS, then resuspended in 500 μl of PBS containing 20 μg/ml propidium iodide and 30 μg/ml RNaseA. The cells were vortexed and incubated at 37 °C for 1 h. Flow cytometry was performed on a Becton Dickinson FACScan interfaced to a Cytomation, Inc. Cicero data acquisition system in the UNC Flow Cytometry Facility. Data were analyzed using Summit version 3.1 (Cytomation, Fort Collins, CO).

Molecular Biology—GST fusion proteins containing fragments of PTP-PEST were engineered using PCR to amplify segments of the PTP-PEST open reading frame. Amplified product was inserted into pGEX2TK (Amersham Biosciences) in-frame with the GST coding sequence. Two deletion mutants of PTP-PEST were created, ΔPro4, in which residues 674 through 682 were deleted, and ΔPro5, in which the C-terminal 20 amino acids were deleted. This latter mutation is similar to the ΔCTH mutant of PTP-HSCF/BDP, which deletes the C-terminal 24 amino acids and abolishes PSTPIP binding (11). These were created by amplification of the entire plasmid, except for the sequences to be deleted, followed by blunt end ligation. Point mutations were engineered into PTP-PEST using the QuikChange strategy (Stratagene, La Jolla CA). Sequence analysis was performed on each mutant to verify the intended point mutations/deletions and that no unintended mutations were present. These analyses were performed in the UNC-CH Genome Analysis Facility on a model 3730 DNA Analyzer (PerkinElmer Life Sciences) using the ABI PRISM™ Dye Terminator Cycle Sequencing Ready Reaction kit with AmpliTaq DNA Polymerase, FS (PerkinElmer, Applied Biosystems Division).

Expression of Recombinant Proteins—Expression of the fusion proteins in *Escherichia coli* was induced by incubation with 0.3 mM isopropyl β-D-thiogalactopyranoside for 4–5 h at room temperature. The bacteria were lysed by sonication, and the proteins purified by binding to glutathione-agarose beads. The fusion proteins were quantified by SDS-PAGE and Coomassie Blue staining.

Protein Analysis—Cells were lysed in 1% Triton X-100 lysis buffer (20 mM Tris-HCl, pH 7.5, 150 mM NaCl, 10% glycerol, 1% Triton X-100) or 0.1% Triton X-100 lysis buffer (0.1% Triton X-100, 0.3 M sucrose, 50 mM Tris.HCl (pH 7.5), 100 mM KCl, 1 mM $CaCl_2$, 2.5 mM $MgCl_2$) containing protease and phosphatase inhibitors and the protein concentration determined using the bicinchoninic acid assay (Pierce). Immunoprecipitations were performed using 1–2 mg of protein and 10 μl of polyclonal antiserum or 2 μl of purified antibody. Immune complexes were precipitated using protein A-Sepharose or protein G-Sepharose beads, washed twice with lysis buffer, twice with Tris-buffered saline and boiled in sample buffer. For GST pull-down experiments, 1–2 mg of lysate was precleared with 20 μg of GST bound to glutathione beads for 45 min at 4 °C. The cleared supernatant was then incubated with 10–20 μg of fusion protein immobilized on glutathione beads for 3 h at 4 °C. The beads were washed twice in lysis buffer, twice in Tris-buffered saline and boiled in sample buffer. Immune complexes and proteins bound to GST fusion proteins were analyzed by Western blotting using a variety of primary antibodies, secondary antibodies conjugated to horseradish peroxidase and enhanced chemiluminescence for detection (Amersham Biosciences). Commercially available antibodies against filamin (Chemicon International, Victoria BC) and β-tubulin (Sigma) were used for these analyses. The polyclonal PTP-PEST antiserum used in this study has been described (20).

Mass Spectrometry—Samples were run on an SDS-polyacrylamide gel, and the bands visualized by silver staining. Protein identification by mass spectrometry was done in the Michael Hooker Proteomics Core Facility at UNC-CH. Briefly, the band of interest was excised and digested with trypsin at ~1:50 enzyme/substrate ratio. Tryptic peptides were eluted from the gel, and MALDI analysis was performed on a Bruker Reflex III time-of-flight mass spectrometer (Bruker). The mass spectrum was analyzed using the RADARS bioinformatics program (28).

RESULTS

Identification of a Novel PTP-PEST Binding Partner—The noncatalytic domains of PTPs serve as docking sites for other

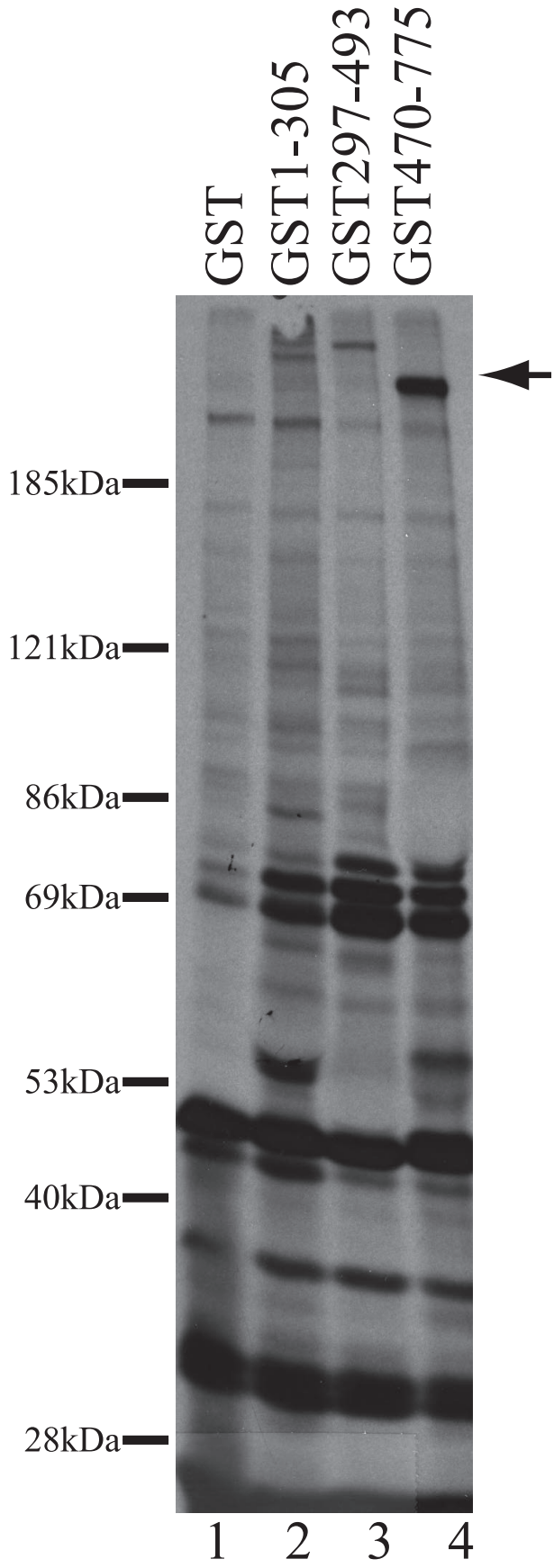

FIGURE 1. **Examination of PTP-PEST-binding proteins.** 293 cells were metabolically labeled with [^{35}S]methionine and [^{35}S]cysteine. Cell lysates were precleared by incubation with GST immobilized to glutathione-Sepharose beads, then incubated with the indicated fusion proteins immobilized on glutathione beads for 1 h at 4 °C. After washing, bound proteins were eluted in Laemmli sample buffer and segregated by SDS-PAGE. Bands were detected by fluorography. The positions of molecular mass markers are indicated on the *left*. The *arrow* denotes the ~280 kDa protein that specifically bound to residues 470–775 of PTP-PEST.

proteins including substrates (29). Whereas a number of substrates and adaptor proteins are known to bind the C-terminal noncatalytic domain of PTP-PEST, it seems likely that additional binding partners remain to be identified. As a first step in the identification of novel binding partners, recombinant GST fusion proteins containing three different fragments of PTP-PEST, immobilized on glutathione-agarose beads, were incubated with lysates of HEK 293 cells metabolically labeled with [^{35}S]methionine and [^{35}S]cysteine. After washing, bound proteins were segregated by SDS-PAGE and visualized by fluorography. A number of proteins bound to all of the fusion proteins including the GST negative control. Each of the regions of PTP-PEST bound uniquely to several proteins. The catalytic domain of PTP-PEST (amino acids 1–305) specifically bound to four proteins with molecular masses of 300, 90, 68, and 55 kDa. The N-terminal region of the noncatalytic domain, containing amino acids 297–493, bound specifically to two proteins, a 305 and an 80 kDa proteins. The most striking associated protein was the 280-kDa protein that uniquely bound to the fusion protein containing the C-terminal region of the noncatalytic domain, containing amino acids 470–775 (Fig. 1). Two additional proteins of molecular mass 80 and 58 kDa were also associated with this fusion protein. A proteomics approach was chosen to pursue the identity of novel PTP-PEST binding partners. Twenty milligrams of HEK 293 cell lysate were incubated with 600 μg of GST fusion protein immobilized on glutathione-agarose beads. The beads were washed, bound proteins eluted with sample buffer and run on a preparative SDS-polyacrylamide gel. Proteins were visualized by silver staining. The 280-kDa protein was again found to associate with the fusion protein containing amino acids 471–775 of PTP-PEST, but was not found in complex with other fusion proteins (data not shown). The protein band was excised and subjected to in-gel trypsin digestion. Peptides were eluted from the gel and analyzed by matrix-assisted laser desorption/ionization mass spectrometry at the Michael Hooker Proteomics Core Facility at UNC-CH. The spectrum of the 280-kDa PTP-PEST associated protein was analyzed using the RADARS bioinformatics software and identified as filamin-A (expectation value 4.3×10^{-5}, 13% peptide coverage). Thus, based upon its mass fingerprint, PTP-PEST appeared to associate with filamin (also known as actin-binding protein (ABP-280).

Validation That Filamin Binds PTP-PEST—To validate the finding that filamin binds PTP-PEST, GST pull-down and co-immunoprecipitation experiments were performed. Lysates of HEK 293 cells were incubated with GST alone or GST-PTP-PEST fusion proteins, which were immobilized on glutathione beads. The beads were washed and bound filamin was detected by Western blotting. Whereas filamin did not bind to GST alone, filamin was associated with the fragment of PTP-PEST extending from residue 470–775 (Fig. 2*A*). This result validated the identification of filamin as a binding partner of recombinant

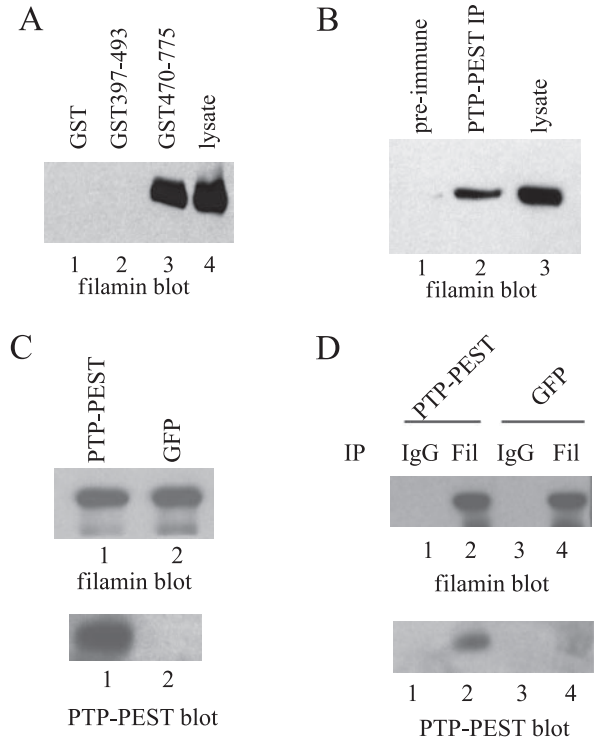

FIGURE 2. **Validation of filamin as a PTP-PEST binding partner.** *A*, 293 cells lysates were incubated with GST (*lane 1*) or GST fusion proteins containing the indicated residues of PTP-PEST (*lanes 2* and *3*). After washing, bound filamin was detected by Western blotting. 50 μg of lysate was run as a control (*lane 4*). *B*, 293 cell lysates were incubated with a PTP-PEST polyclonal antiserum (*lane 2*) or the preimmune serum (*lane 1*). Immune complexes were collected using protein A-Sepharose, washed, and bound filamin detected by Western blotting. Lysate was run as a control (*lane 3*). *C*, HeLa cells were infected with Ad-GFP or Ad-PTP-PEST at an m.o.i. of 30 and the cells lysed at 24-h postinfection. 10 μg of lysate were analyzed for PTP-PEST expression by Western blotting using PTP-PEST polyclonal antiserum. *D*, 1 mg of lysate was incubated with incubated with filamin monoclonal (*lanes 2* and *4*) or isotype control (*lanes 1* and *3*) antibodies. Immune complexes were collected using protein G-Sepharose, washed, and bound PTP-PEST detected by Western blotting.

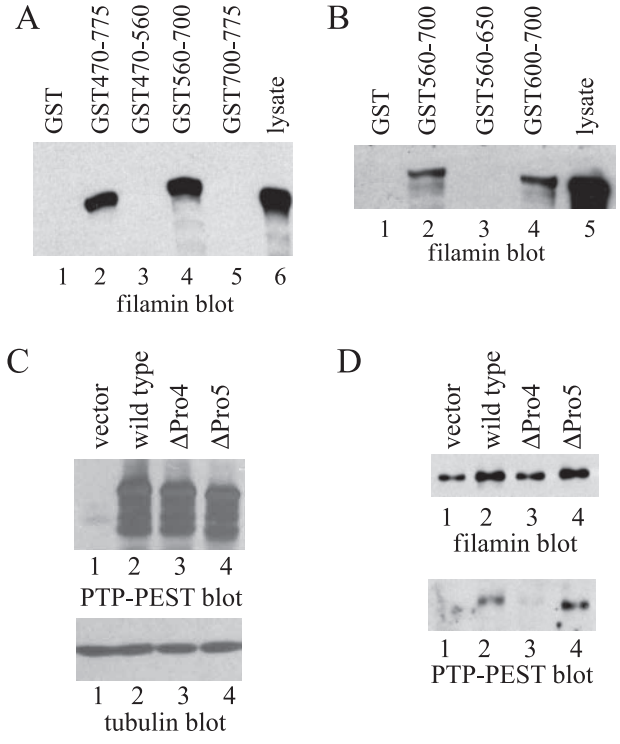

FIGURE 3. **The Pro4 region of PTP-PEST mediates filamin binding.** *A*, 293 cell lysate was precleared with GST, then incubated with GST alone (*lane 1*) or GST fused to the indicated amino acids of PTP-PEST (*lanes 2–5*). After washing bound filamin was detected by Western blotting. 25 μg of lysate were loaded as a control (*lane 6*). *B*, as in *A*, the indicated fragments of PTP-PEST fused to GST (*lanes 2–4*) were incubated with 293 cell lysate and bound filamin detected by blotting. 25 μg of lysate were loaded as a control (*lane 5*). *C* and *D*, 293 cells were transiently transfected with the empty pEYFP vector (*lane 1*), or plasmids encoding YFP fusion proteins containing wild-type PTP-PEST (*lane 2*), ΔPro4 (*lane 3*), or ΔPro5 (*lane 4*). 25 μg of lysate was blotted for PTP-PEST or β-tubulin as a loading control (*C*). Filamin was immunoprecipitated from cell lysates, and the immune complexes blotted for filamin (*D*, *top*) or PTP-PEST (*D*, *bottom*).

PTP-PEST. To further verify this interaction, endogenous PTP-PEST was immunoprecipitated from HEK 293 lysates using a polyclonal antiserum and the immune complex analyzed by Western blotting with a filamin antibody. Endogenous filamin was detected in the PTP-PEST immune complex, but was not detected in preimmune control immunoprecipitations (Fig. 2*B*). The reciprocal co-immunoprecipitation experiments were performed using lysates of Hela cells infected with adenoviruses designed to express GFP or PTP-PEST (Fig. 2*C*). Filamin was immunoprecipitated and the immune complex blotted for associated PTP-PEST using the polyclonal antiserum (Fig. 2*D*). PTP-PEST was detected in the filamin immune complex from PTP-PEST-expressing cells, but was not found in the isotype control immune complex (Fig. 2*D*). A small amount of PTP-PEST could be detected in filamin immune complexes from GFP-expressing cells. This reflected interaction between endogenous PTP-PEST and filamin (Fig. 2*D*). These reciprocal co-immunoprecipitations suggest that filamin is a *bona fide* binding partner of PTP-PEST and that the two proteins are likely to associate *in vivo*.

Identification of the Filamin Binding Site on PTP-PEST—To map the region of PTP-PEST required for filamin binding, GST fusion proteins containing different fragments of PTP-PEST were used. Lysates were incubated with fusion proteins immobilized to glutathione-agarose beads and bound filamin was detected by Western blotting. A recombinant protein containing amino acids 560–700 of PTP-PEST bound filamin, whereas fusion proteins containing PTP-PEST residues 471–560 or 700–775 did not (Fig. 3*A*). This experiment narrowed the filamin binding site to within residues 560–700 of PTP-PEST. Two additional fusion proteins encoding residues 560–650 and 600–700 were tested for filamin binding. The former failed to bind filamin, whereas the latter was able to bind filamin (Fig. 3*B*). This finding suggested that the filamin binding site on PTP-PEST was likely between residues 650 and 700, a region that contains the fourth proline-rich sequence of PTP-PEST, Pro4. As numerous proteins dock to PTP-PEST via proline-rich sequences in its C-terminal noncatalytic domain, Pro4 appeared as a good candidate binding site for filamin. To test this hypothesis, a 9-amino acid deletion removing Pro4 was engineered into full-length PTP-PEST (ΔPro4). For this experiment, PTP-PEST constructs were transiently expressed in HEK 293 cells as yellow fluorescent protein (YFP) fusion proteins to assess the ability of these mutants to co-immunoprecipitate with endogenous filamin. YFP-PTP-PEST, YFP-ΔPro4, and YFP-ΔPro5 (a mutation deleting the C-terminal 20 resi-

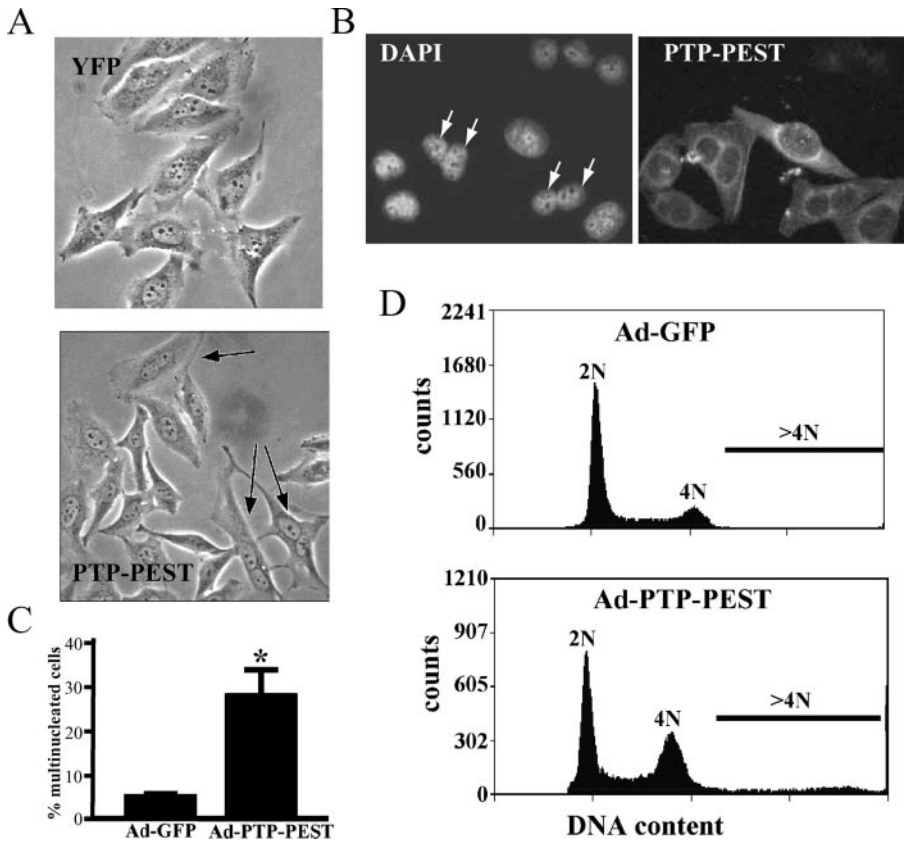

FIGURE 4. **Expression of PTP-PEST induces a multinucleated phenotype in HeLa cells.** *A*, HeLa cells were transfected with YFP or YFP-PTP-PEST, selected with G418 and sorted by FACS. The cells were visualized by phase contrast microscopy. *Arrows* denote multinucleated cells in the YFP-PTP-PEST population. *B*, HeLa cells were infected with Ad-PTP-PEST at an m.o.i. of 10 and the cells analyzed 48-h postinfection. Cells were fixed and stained with a PTP-PEST monoclonal antibody to identify infected cells and with DAPI to mark nuclei. *Arrows*/*arrowheads* denote multiple nuclei in a single cell. *C*, HeLa cells were infected with Ad-GFP or Ad-PTP-PEST at an m.o.i. of 30, and the cells analyzed 72-h postinfection. Cells were stained with a β-tubulin antibody as a cytoplasmic marker and with DAPI to mark nuclei. Three slides were scored per infection and greater than 50 cells were scored per slide. The percentage of multinucleated cells was determined, and the average of three experiments (±S.E.) is shown. The data were analyzed using an unpaired, one-tailed Student's *t* test (*, $p < 0.01$). *D*, cells infected with Ad-GFP or Ad-PTP-PEST at an m.o.i. of 30 for 72 h were fixed, stained with propidium iodide, and analyzed for DNA content by flow cytometry. The DNA peaks corresponding to 2N and 4N are indicated, as is the region where DNA content is greater than 4N. The results of a single representative experiment, out of four total experiments, are shown.

dues which contains Pro5) were expressed to similar levels, as detected by Western blotting (Fig. 3*C*). Filamin was immunoprecipitated from lysates and associated PTP-PEST detected by Western blotting using a PTP-PEST polyclonal antibody. Whereas YFP-PTP-PEST and YFP-ΔPro5 were co-immunoprecipitated with filamin, the YFP-ΔPro4 mutant was defective for filamin binding (Fig. 3*D*). This result supports the contention that this proline-rich region is the site of interaction between PTP-PEST and filamin.

PTP-PEST Expression Induces a Multinucleated Phenotype—HeLa cell populations stably expressing PTP-PEST variants as YFP fusion proteins were established by drug selection and sorting by FACS. Examination of wild-type YFP-PTP-PEST-expressing HeLa cells revealed a high frequency of cells with a multinucleated phenotype (Fig. 4*A*). This phenotype is intriguing, given the reported role of PTP-PEST in controlling cytokinesis (5). The wild-type YFP-PTP-PEST-expressing cells exhibited a severe cell proliferation defect that resulted in a rapid loss of protein expression (data not shown). The multinucleated phenotype was recapitulated using two different methods of transient expression; infection with adenoviral vectors and transient expression of YFP fusion proteins. HeLa cells were infected with an adenovirus designed to express GFP (Ad-GFP), which served as a negative control, or with the adenovirus-PTP-PEST (Ad-PTP-PEST). Seventy-two hours postinfection, nuclei were stained with DAPI, and the cells visualized by immunofluorescence using a PTP-PEST or a β-tubulin antibody, or by visualizing GFP fluorescence. Ad-GFP-infected cells were rarely observed to contain more than a single nucleus, whereas Ad-PTP-PEST infected cells were frequently observed to contain multiple nuclei (Fig. 4*B*). Multinucleated cells were scored in multiple experiments and expressed as percentage of cells containing multiple nuclei. Whereas a small percentage of control cell populations contained more than a single nucleus, ~25% of the Ad-PTP-PEST-infected cells were multinucleated (Fig. 4*C*). This phenotype was further validated by examining the ploidy of Ad-GFP and Ad-PTP-PEST infected cells by flow cytometry. Asynchronously growing cells were fixed, stained with propidium iodide, and analyzed by flow cytometry. Control cells exhibited the typical profile of cycling cells with a peak of cells with 2N DNA content, a peak of cells with 4N DNA content and a population of cells with DNA content between 2N and 4N indicative of cells in S phase (Fig. 4*D*). Ad-PTP-PEST cells exhibited the same basic profile with two notable differences. First, the ratio of cells with 4N DNA content to cells with 2N DNA content was increased. Second, there was a population of cells with greater than 4N DNA content that was not present in the control cells. The flow cytometric analysis also supports the finding that PTP-PEST-expressing cells exhibit a higher frequency of multiple nuclei.

The Pro4 Region Is Required to Induce the Multinucleated Phenotype—To begin to address the mechanism by which PTP-PEST generates a multinuclear phenotype, mutants of PTP-PEST were analyzed for their ability to induce this phenotype. YFP-PTP-PEST fusion proteins were transiently expressed in HeLa cells. Seventy-two hours post-transfection, cells were fixed, and stained with DAPI, and cells examined by fluorescent microscopy. Cells expressing exogenous protein were identified as YFP-positive cells and the number of nuclei per YFP-positive cell counted (Fig. 5*A*). Less than 5% of control cells, expressing the empty YFP vector, exhibited multiple nuclei.

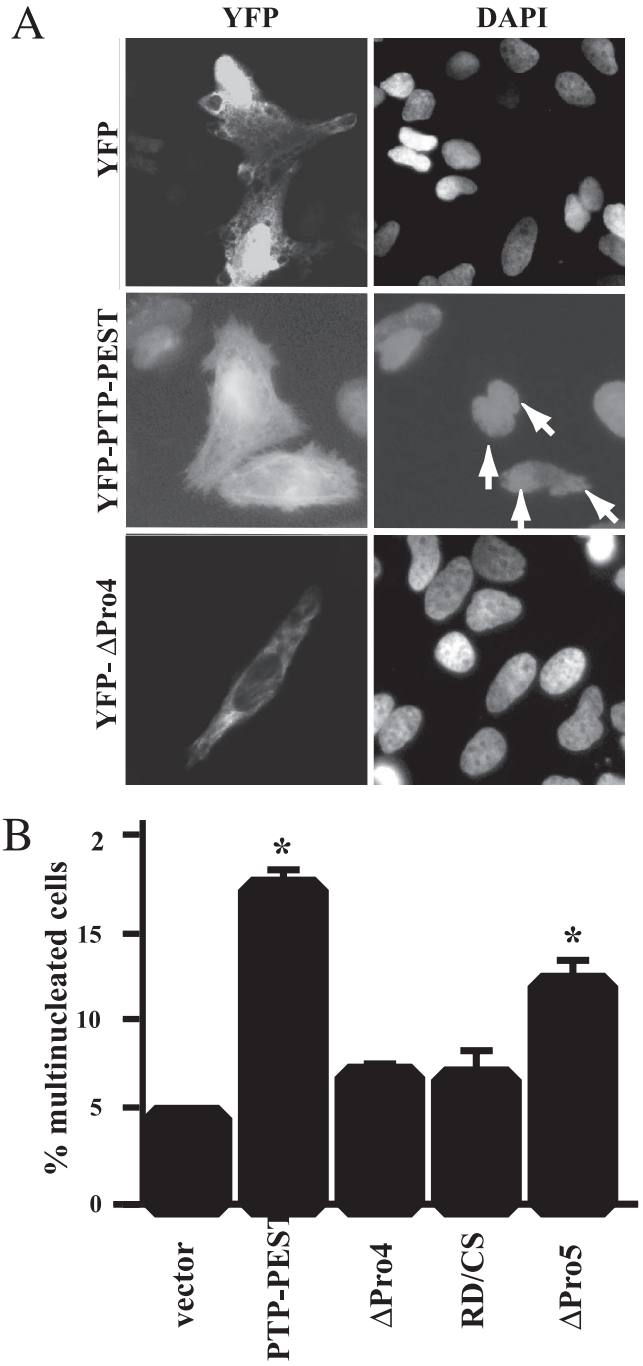

FIGURE 5. **The Pro4 region of PTP-PEST is required to induce the multinucleated phenotype.** Cells were transiently transfected with the empty pEYFP vector or plasmids encoding YFP fusion proteins containing wild-type or mutant PTP-PEST sequences. Seventy-two hours post-transfection, the cells were fixed and stained with DAPI. *A*, images of the vector, YFP-PTP-PEST (wild type) and YFP-PTP-PEST ΔPro4-transfected cells are shown. Transfected cells were identified as YFP-positive cells by fluorescent microscopy (*left panels*), and the number of nuclei per YFP-positive cell scored (*right panels*). *Arrows* denote two YFP-PTP-PEST-positive cells (*left panel*) containing two nuclei each (*right panel*). *B*, percentage of multinucleated cells expressing the empty vector or various PTP-PEST constructs was determined. The cells on three slides were scored in each experiment and greater than 50 expressing cells scored per slide. The results from at least three experiments were averaged and plotted (±S.E.). The data were analyzed using a one-way analysis of variance ($p < 0.0001$). The data were further analyzed using Dunnett's multiple comparison test (comparison *versus* vector; * denotes $p < 0.01$).

Approximately 17% of the YFP-PTP-PEST-expressing cells exhibited the multinucleated phenotype (Fig. 5*B*). Thus the results obtained using adenovirus to express exogenous PTP-PEST were recapitulated using transient transfection of YFP fusion proteins. To address the role of phosphatase activity in inducing the formation of multinucleated cells, a catalytically defective mutant was used. Two mutations were engineered into PTP-PEST, C231S, which removes the catalytic cysteine and abolishes activity, and R237D, which dramatically reduces the affinity of phosphatases for their substrates (30, 31). This latter mutation ensured that the mutant would not exhibit neomorphic effects because of substrate trapping *in vivo*. In contrast to YFP-PTP-PEST, YFP-RD/CS induced a multinucleated phenotype in ~6% of cells, which was not statistically different from the level seen in control cells (Fig. 5*B*). This result demonstrates that catalytic activity is essential for induction of the phenotype. The two PTP-PEST binding partners most likely involved in controlling cell division are filamin and PSTPIP. To address the importance of these interactions, the ΔPro4 and ΔPro5 mutants were tested for their ability to produce multinucleated cells. The ΔPro5 mutant was engineered to mimic the previously published mutation deleting the CTH region of PTP-PEST family of PTPs, which disrupts PSTPIP binding (11). YFP-ΔPro4-expressing cells contained ~6% multinucleated cells, which again was not significantly different from the frequency seen in control cells, demonstrating that the Pro4 sequence was required for PTP-PEST to induce this phenotype (Fig. 5*B*). Expression of YFP-ΔPro5 in cells produced a multinucleated phenotype in ~12% of the cells. This result is statistically different from both the vector control cells (Tukey's Multiple Comparison Test, $p < 0.001$) and wild-type-expressing cells ($p < 0.01$). This result suggests that both the Pro4 and Pro5 regions function in controlling this phenotype, and that the Pro4 region is essential for inducing multinucleation.

If the PTP-PEST/filamin complex was biologically significant during cytokinesis, it was postulated that cells devoid of filamin-A would be resistant to PTP-PEST-induced multinucleation. A filamin-A-deficient human melanoma cell line (M2) and a derivative re-expressing wild-type filamin (A7) (32) seemed appropriate for these studies. However, the M2 cells exhibited a multinucleated phenotype (>20%) while A7 cells were predominantly mononuclear (data not shown). These findings preclude the use of the M2 cells to address this question. As an alternative strategy, filamin-A expression in HeLa cells was reduced using siRNA (Fig. 6*A*). It was only possible to partially deplete filamin-A in transfected HeLa cells and following transfection, cells expressing high levels of filamin-A, and cells with suppressed levels of filamin-A were clearly distinguished by immunofluorescence (Fig. 6*B*). siRNA-mediated knockdown of filamin did not cause a significant change in the degree of multinucleation of HeLa cells (3.3 ± 0.9%) in comparison to control HeLa cells (2.0 ± 0.35%), possibly because of the incomplete inhibition of expression.

Optimum siRNA-mediated suppression of filamin levels was at 72 h, and could be maintained beyond 120 h, while optimum expression of YFP-PTP-PEST fusion constructs was at 72 h. Hence, HeLa cells were transfected with filamin siRNA and 48 h later the cells were transfected with plasmids encoding the YFP

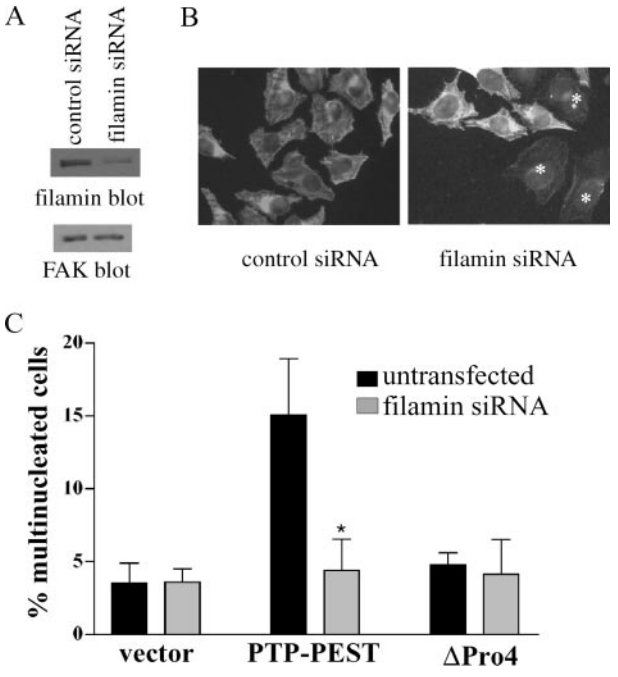

FIGURE 6. **The PTP-PEST-induced multinucleated phenotype is reduced in filamin siRNA-treated cells.** *A*, HeLa cells were transfected with filamin-A or control siRNA. After 72 h, the cells were lysed and analyzed by Western blotting for filamin or FAK as a loading control. *B*, cells treated as in *A* were stained for filamin to identify cells transfected with filamin siRNA. *Stars* denote cells with reduced filamin levels relative to control cells. *C*, HeLa cells were transiently transfected with filamin siRNA. Forty-eight hours later the cells were transiently transfected with the empty pEYFP vector or plasmids encoding YFP fusion proteins containing wild type or ΔPro4 mutant PTP-PEST sequences. 72 h post-transfection, the cells were fixed and stained for filamin and DAPI. The percentage of multinucleated cells expressing the empty vector or PTP-PEST constructs was determined in cells with normal (untransfected) and reduced (filamin siRNA) filamin expression. Between 100 and 200 total cells were scored in each experiment for each YFP construct. The results from three experiments were averaged and plotted (±S.E.). The data were analyzed using an unpaired, one-tailed Student's *t* test to compare data from untransfected and filamin siRNA transfected cells (*, $p < 0.05$).

fusion proteins. The multinucleated phenotype was assessed 72 h following transfection with the GFP plasmids. The cells were fixed and stained for filamin-A to identify cells expressing high and low levels of filamin-A. The nuclear phenotype of YFP-positive cells was scored (Fig. 6*C*). In cells containing normal levels of filamin-A, 15% of YFP-PTP-PEST-expressing cells were multinucleated. In contrast, the frequency of multinucleated YFP-PTP-PEST-expressing cells was reduced to 5% in cells with depleted filamin (Fig. 6*C*). The proportion of control YFP-expressing cells exhibiting a multinucleated phenotype was similar in cells exhibiting normal or depleted levels of filamin-A and was not different to the proportion seen in untransfected HeLa cells, *i.e.* <5%. Furthermore, cells expressing the filamin-binding defective PTP-PEST mutant (ΔPro4) exhibited similar proportions of multinucleated cells as control cells with either normal or suppressed levels of filamin. These results support the hypothesis that the interaction between PTP-PEST and filamin is important for the induction of the multinucleated phenotype by PTP-PEST.

DISCUSSION

In this article, we have identified filamin as a novel binding partner for PTP-PEST. Whereas it is not yet clear if this reflects a direct or indirect interaction, the Pro4 sequence within PTP-PEST is required for the interaction. Establishing cells stably expressing exogenous PTP-PEST proved difficult apparently because of a growth defect and early passage HeLa cells stably expressing PTP-PEST had an increased propensity for multinucleation. The selective disadvantage conferred by PTP-PEST-expressing cells led to rapid loss of protein expression. The multinucleated phenotype was also induced in HeLa cells when PTP-PEST was expressed using an adenoviral vector or transiently expressed as a YFP fusion protein.

It has been reported that PTP-PEST-null cells also exhibit a cytokinesis defect as pairs of cells joined by an actin-rich remnant of the cleavage furrow are frequently observed (5). At first glance the findings that exogenous PTP-PEST expression and ablation of PTP-PEST expression produce a similar phenotype are counterintuitive, *i.e.* that gain of function and loss of function result in similar phenotypes. Interestingly, similar seemingly disparate results between null cells and cells expressing exogenous PTP-PEST are observed in the motility of cells (5, 8). Cells expressing exogenous PTP-PEST exhibit reduced cell motility, as do PTP-PEST-null fibroblasts. These observations can be reconciled if cycles of tyrosine phosphorylation/dephosphorylation are required to regulate these biological processes. Cells expressing exogenous protein exhibit insufficient phosphorylation of key substrates, and thus a failure to regulate function resulting in defective cytokinesis. Conversely, null cells exhibit constitutive phosphorylation of key substrates and thus a failure to regulate function resulting in defective cytokinesis.

The PTP-PEST mutant that exhibits deficient filamin binding (ΔPro4) does not induce a multinucleated phenotype implicating a Pro4 binding partner in the induction of this phenotype. Pro4 is a binding site for three different proteins, Grb2, Csk, and filamin (12, 18, 19). It is quite unlikely that Grb2 is the relevant Pro4 binding partner associated with this phenotype as Grb2 can associate with three additional proline-rich sequences in the C-terminal non-catalytic domain of PTP-PEST (12). Csk is a second Pro4 binding partner (18, 19), and the major cellular function of this tyrosine kinase is to negatively regulate the catalytic activity of the Src family of tyrosine kinases (33). The c-Src kinase is activated during mitosis (34) and inhibition of Src family kinases blocks the initiation of cytokinesis (35, 36). However, PTPα, rather than Csk, appears to be the major enzyme regulating phosphorylation of the negative regulatory site during mitosis (37). The third Pro4 binding partner that could function in the control of cytokinesis is filamin. A role for filamin in cytokinesis has been inferred by its localization to the cleavage furrow/midbody (38). This original finding was recently confirmed in a proteomics study identifying filamin as a component of isolated midbodies, although RNAi-mediated knockdown of filamin did not induce a cytokinesis phenotype in *Caenorhabditis elegans* (39). Because the induction of a multinucleated phenotype by PTP-PEST requires filamin-A expression, filamin-A is the most likely known Pro4-docking protein controlling this phenotype.

The catalytic activity of PTP-PEST is required to promote the multinucleated phenotype, suggesting that dephosphorylation of select substrates is necessary to alter cell division. Filamin has been reported as a substrate for tyrosine phosphorylation by Lck *in vitro* (40), but we have been unable to detect phosphotyrosine changes on filamin upon transient expression of PTP-PEST (data not shown). It seems more likely that this interaction serves to localize a fraction of the cellular PTP-PEST in the vicinity of other proteins, which serve as direct substrates. There is recent evidence for the involvement of phosphotyrosine-containing proteins during cytokinesis. Tyrosine-phosphorylated proteins have been found to accumulate in cleavage furrows in sea urchin embryos (41). The molecular targets for tyrosine phosphorylation in regulation of cytokinesis have not been conclusively established and the relevant PTP-PEST substrates are unknown. There are a number of reasons why RhoGAPs or RhoGEFs are currently the favored targets. Filamin-A, which can in turn associate with Rho (26), may act as a scaffold to tether these proteins in complex to facilitate regulation. PTP-PEST has already been implicated as a regulator of Rac in fibroblasts (9, 10). Trio is an exchange factor for Rho that associates with filamin-A and is tyrosine-phosphorylated, but it is unclear if its activity is regulated by phosphorylation (42, 43). Vav3 is a RhoGEF that is regulated in a cell cycle-dependent manner in HeLa cells and constitutive expression of Vav3 promotes a multinucleated phenotype (44). Tyrosine phosphorylation of the regulatory region of the Vav family of GEFs promotes a conformational change and activation of catalytic activity (45). Mutation of this tyrosine to phenylalanine in Vav3 (tyrosine 173) abolishes its ability to induce multinucleated cells, indirectly suggesting that catalytic activity is required to promote this phenotype (44). The activity of p190RhoGAP is regulated *in vivo* by tyrosine phosphorylation (46). P190RhoGAP has been localized to the region of the cleavage furrow in dividing cells and overexpression of p190RhoGAP induces a multinucleated phenotype (47). Clearly there are a number of plausible mechanisms via which PTP-PEST could serve to regulate cytokinesis. Future studies will focus upon the elucidation of molecular targets and the detailed mechanism of how PTP-PEST controls cytokinesis.

Acknowledgments—We thank Joan Taylor and Mark Sussman for providing key reagents for this study. We are particularly indebted to Ted Salmon and Daniella Cimini for the use of their equipment and their assistance in time-lapse video microscopy. Nancy Martin provided assistance with the flow cytometry experiments. Thanks also to members of the laboratory for useful discussions during the course of this study and to Michelle King and Alison Worsham for their technical assistance.

REFERENCES

1. Alonso, A., Sasin, J., Bottini, N., Friedberg, I., Friedberg, I., Osterman, A., Godzik, A., Hunter, T., Dixon, J., and Mustelin, T. (2004) *Cell* **117,** 699–711
2. Cheng, J., Daimaru, L., Fennie, C., and Lasky, L. A. (1996) *Blood* **88,** 1156–1167
3. Kim, Y. W., Wang, H., Sures, I., Lammers, R., Martell, K. J., and Ullrich, A. (1996) *Oncogene* **13,** 2275–2279
4. Matthews, R. J., Bowne, D. B., Flores, E., and Thomas, M. L. (1992) *Mol. Cell Biol.* **12,** 2396–2405
5. Angers-Loustau, A., Cote, J. F., Charest, A., Dowbenko, D., Spencer, S., Lasky, L. A., and Tremblay, M. L. (1999) *J. Cell Biol.* **144,** 1019–1031
6. Badour, K., Zhang, J., Shi, F., Leng, Y., Collins, M., and Siminovitch, K. A. (2004) *J. Exp. Med.* **199,** 99–112
7. Mustelin, T., Vang, T., and Bottini, N. (2005) *Nat. Rev. Immunol.* **5,** 43–57
8. Garton, A. J., and Tonks, N. K. (1999) *J. Biol. Chem.* **274,** 3811–3818
9. Sastry, S. K., Lyons, P. D., Schaller, M. D., and Burridge, K. (2002) *J. Cell Sci.* **115,** 4305–4316
10. Sastry, S. K., Rajfur, Z., Liu, B. P., Cote, J. F., Tremblay, M. L., and Burridge, K. (2006) *J. Biol. Chem.* **281,** 11627–11636
11. Spencer, S., Dowbenko, D., Cheng, J., Li, W., Brush, J., Utzig, S., Simanis, V., and Lasky, L. A. (1997) *J. Cell Biol.* **138,** 845–860
12. Charest, A., Wagner, J., Kwan, M., and Tremblay, M. L. (1997) *Oncogene* **14,** 1643–1651
13. Habib, T., Herrera, R., and Decker, S. J. (1994) *J. Biol. Chem.* **269,** 25243–25246
14. Garton, A. J., Burnham, M. R., Bouton, A. H., and Tonks, N. K. (1997) *Oncogene* **15,** 877–885
15. Shen, Y., Schneider, G., Cloutier, J. F., Veillette, A., and Schaller, M. D. (1998) *J. Biol. Chem.* **273,** 6474–6481
16. Cote, J. F., Turner, C. E., and Tremblay, M. L. (1999) *J. Biol. Chem.* **274,** 20550–20560
17. Nishiya, N., Iwabuchi, Y., Shibanuma, M., Cote, J. F., Tremblay, M. L., and Nose, K. (1999) *J. Biol. Chem.* **274,** 9847–9853
18. Davidson, D., Cloutier, J. F., Gregorieff, A., and Veillette, A. (1997) *J. Biol. Chem.* **272,** 23455–23462
19. Cloutier, J. F., and Veillette, A. (1996) *EMBO J.* **15,** 4909–4918
20. Shen, Y., Lyons, P., Cooley, M., Davidson, D., Veillette, A., Salgia, R., Griffin, J. D., and Schaller, M. D. (2000) *J. Biol. Chem.* **275,** 1405–1413
21. Cong, F., Spencer, S., Cote, J. F., Wu, Y., Tremblay, M. L., Lasky, L. A., and Goff, S. P. (2000) *Mol. Cell* **6,** 1413–1423
22. Cote, J. F., Chung, P. L., Theberge, J. F., Halle, M., Spencer, S., Lasky, L. A., and Tremblay, M. L. (2002) *J. Biol. Chem.* **277,** 2973–2986
23. van der Flier, A., and Sonnenberg, A. (2001) *Biochim. Biophys. Acta* **1538,** 99–117
24. Stossel, T. P., Condeelis, J., Cooley, L., Hartwig, J. H., Noegel, A., Schleicher, M., and Shapiro, S. S. (2001) *Nat. Rev. Mol. Cell Biol.* **2,** 138–145
25. Marti, A., Luo, Z., Cunningham, C., Ohta, Y., Hartwig, J., Stossel, T. P., Kyriakis, J. M., and Avruch, J. (1997) *J. Biol. Chem.* **272,** 2620–2628
26. Ohta, Y., Suzuki, N., Nakamura, S., Hartwig, J. H., and Stossel, T. P. (1999) *Proc. Natl. Acad. Sci. U. S. A.* **96,** 2122–2128
27. Graham, F. L., and van der Eb, A. J. (1973) *Virology* **52,** 456–467
28. Field, H. I., Fenyo, D., and Beavis, R. C. (2002) *Proteomics.* **2,** 36–47
29. Tonks, N. K., and Neel, B. G. (2001) *Curr. Opin. Cell Biol.* **13,** 182–195
30. Flint, A. J., Tiganis, T., Barford, D., and Tonks, N. K. (1997) *Proc. Natl. Acad. Sci. U. S. A.* **94,** 1680–1685
31. Streuli, M., Krueger, N. X., Thai, T., Tang, M., and Saito, H. (1990) *EMBO J.* **9,** 2399–2407
32. Flanagan, L. A., Chou, J., Falet, H., Neujahr, R., Hartwig, J. H., and Stossel, T. P. (2001) *J. Cell Biol.* **155,** 511–517
33. Cole, P. A., Shen, K., Qiao, Y., and Wang, D. (2003) *Curr. Opin. Chem. Biol.* **7,** 580–585
34. Chackalaparampil, I., and Shalloway, D. (1988) *Cell* **52,** 801–810
35. Roche, S., Fumagalli, S., and Courtneidge, S. A. (1995) *Science* **269,** 1567–1569
36. Moasser, M. M., Srethapakdi, M., Sachar, K. S., Kraker, A. J., and Rosen, N. (1999) *Cancer Res.* **59,** 6145–6152
37. Zheng, X. M., and Shalloway, D. (2001) *EMBO J.* **20,** 6037–6049
38. Nunnally, M. H., D'Angelo, J. M., and Craig, S. W. (1980) *J. Cell Biol.* **87,** 219–226
39. Skop, A. R., Liu, H., Yates, J., III, Meyer, B. J., and Heald, R. (2004) *Science* **305,** 61–66

40. Sharma, C. P., and Goldmann, W. H. (2004) *Cell Biol. Int.* **28,** 935–941
41. Ng, M. M., Chang, F., and Burgess, D. R. (2005) *Dev. Cell* **9,** 781–790
42. Bellanger, J. M., Astier, C., Sardet, C., Ohta, Y., Stossel, T. P., and Debant, A. (2000) *Nat. Cell Biol.* **2,** 888 – 892
43. Medley, Q. G., Buchbinder, E. G., Tachibana, K., Ngo, H., Serra-Pages, C., and Streuli, M. (2003) *J. Biol. Chem.* **278,** 13265–13270
44. Fujikawa, K., Inoue, Y., Sakai, M., Koyama, Y., Nishi, S., Funada, R., Alt, F. W., and Swat, W. (2002) *Proc. Natl. Acad. Sci. U. S. A.* **99,** 4313– 4318
45. Turner, M., and Billadeau, D. D. (2002) *Nat. Rev. Immunol.* **2,** 476 – 486
46. Haskell, M. D., Nickles, A. L., Agati, J. M., Su, L., Dukes, B. D., and Parsons, S. J. (2001) *J. Cell Sci.* **114,** 1699 –1708
47. Su, L., Agati, J. M., and Parsons, S. J. (2003) *J. Cell Biol.* **163,** 571–582